

TECHNICAL NOTE

## Inclusion of higher-temperature effects in a soil behaviour model

H. R. THOMAS\*, S. SIDDIQUA\* and S. C. SEETHARAM\*

This technical note presents a coupled thermo-hydro-mechanical model for unsaturated soil, which can be applied in the context of high temperature. A new pore gas or bulk air transfer equation is introduced. Additionally the effect of temperature on the latent heat of vapourisation and specific heat capacities is incorporated. Adsorbed water is also included. The performance of the model is demonstrated via the simulation of a high temperature (150°C) thermo-hydraulic-mechanical experiment carried out on a column of MX-80 bentonite by Commissariat à l’Energie Atomique, France. The model showed good correlation of experimental and numerical results.

**KEYWORDS:** model tests; temperature effects

Cette communication technique présente un modèle thermo-hydrromécanique accouplé pour les sols non saturés, pouvant être appliqué dans le contexte de températures élevées. On introduit une équation nouvelle de transfert de gaz interstitiel ou d’air en vrac. En outre, on incorpore également l’effet de la température sur la chaleur de vaporisation latente et les chaleurs massiques, ainsi que l’eau adsorbée. Les performances du modèle sont démontrées par la simulation d’une expérience thermo-hydrromécanique à température élevée (150°C) effectuée sur une colonne de bentonite MX-80 par le Commissariat à l’Énergie Atomique en France. Le modèle représenté présente une bonne corrélation des résultats expérimentaux et numériques.

### INTRODUCTION

The study of coupled thermal, hydraulic and mechanical behaviour of unsaturated soils is a complex problem in the field of geoenvironmental engineering (Thomas, 2006). Practical applications include geothermal engineering, high-level nuclear waste repository design and landfill engineering. A few of these practical problems involve high-temperature conditions, defined for the purposes of this note as temperatures in excess of 100°C. Such temperatures can cause intense drying of porous media.

In recent years, a number of thermo-hydro-mechanical models have been proposed (e.g. Thomas & He, 1995; Olivella *et al.*, 1996), based on a mechanistic approach that considers conservation laws coupled with constitutive relationships. For the thermo-hydraulic part, the models principally follow Philip & de Vries (1957). Previous work has focused on problems involving temperatures lower than 100°C. Olivella & Gens (2000), however, presented a formulation where the effect of higher temperatures on vapour pressure due to phase change was analysed in the context of low-permeability clays.

The principal objective of this note is to present a model that can be applied in the context of high temperature. The starting point is the approach presented by Thomas & He (1997). A new pore gas or bulk air transfer equation is introduced (Luikov, 1966). Additionally, the effect of temperature on the latent heat of vaporisation and specific heat capacities is incorporated. Adsorbed water is also included. In order to investigate the performance of the model, an experiment carried out by Commissariat à l’Energie Atomique (CEA), France on MX80 bentonite column has been chosen (Gatabin & Billaud, 2005).

### THEORETICAL FRAMEWORK

Pore gas is assumed to comprise a mixture of dry air and vapour. Therefore pore gas transfer essentially describes bulk air flow. The mass conservation equation can be expressed as (Luikov, 1966)

$$\frac{\partial}{\partial t} [\rho_g \theta_g] + \frac{\partial}{\partial t} [\rho_g H \theta_l] = -\nabla \cdot \mathbf{J}_g + S \quad (1)$$

where  $t$  is time,  $\rho_g$  is the density of pore gas (or bulk air),  $\theta_g$  is the volumetric gas content =  $n(1 - S_l)$ ,  $n$  is the porosity,  $S_l$  is the degree of saturation of liquid,  $H$  is Henry’s volumetric coefficient of solubility of the gas phase (dry air–vapour mixture),  $\theta_l$  is the volumetric liquid content =  $nS_l$ ,  $\mathbf{J}_g$  is the pore gas flux, and  $S$  is the sink/source term.

The pore gas is assumed to be an ideal gas. Therefore the ideal gas law will be implemented as

$$P_g = \rho_g R_g T \quad (2)$$

where  $R_g$  is the gas constant for the pore gas. The flux term  $\mathbf{J}_g$  considers the flow of pore gas due to the total pressure gradient and due to the transfer of dissolved gas in the liquid phase. Accordingly,  $\mathbf{J}_g$  can be expressed as

$$\mathbf{J}_g = -\nabla \cdot [\rho_g \mathbf{v}_g] - H \nabla \cdot [\rho_g \mathbf{v}_l] \quad (3)$$

where  $\mathbf{v}_g$  is the velocity of pore gas and  $\mathbf{v}_l$  is the liquid velocity. The velocity of pore gas is decomposed so as to consider both total pressure gradient and temperature gradient. Therefore  $\mathbf{v}_g$  can be defined as (Geraminegad & Saxena, 1986)

$$\mathbf{v}_g = -\frac{k_{int} K_{rg}}{\mu_g} \left( \frac{P_g}{T} \nabla T + \nabla P_g \right) \quad (4)$$

where  $k_{int}$  is the intrinsic permeability of the material,  $K_{rg}$  is the relative permeability of the gas phase, and  $\mu_g$  is the dynamic viscosity of the pore gas (or bulk air). The dynamic viscosity of the pore gas depends on temperature and the ratio of vapour and air pressures.

Manuscript received 2 May 2008; revised manuscript accepted 1 February 2009.

Discussion on this paper closes on 1 September 2009, for further details see p. ii.

\* Geoenvironmental Research Centre, Cardiff School of Engineering, Cardiff University, Wales, UK.

The sink/source term in equation (1) follows that of Luikov (1966). Based on Philip & de Vries (1957), the flux can be expressed as

$$S = -\rho_g \nabla \cdot \left[ D_{\text{atms}} \tau_v \theta_g \nabla \left( \frac{\rho_v}{\rho_g} \right) \right] \quad (5)$$

where  $D_{\text{atms}}$  is the molecular diffusivity of vapour through air,  $\tau_v$  is the tortuosity factor,  $\rho_v$  is the density of water vapour, and  $\rho_v/\rho_g$  is the vapour fraction.

The combined liquid and water vapour conservation equation can be expressed as

$$\frac{\partial}{\partial t} [\rho_l \theta_l + \rho_v \theta_g] = -\nabla \cdot \left[ \rho_l \mathbf{v}_l - \rho_g D_{\text{atms}} \tau_v \theta_g \nabla \left( \frac{\rho_v}{\rho_g} \right) \right] \quad (6)$$

where  $\rho_l$  is the density of liquid water, which is also considered to be a function of temperature, and all other terms are as described earlier. The right-hand side of equation (6) includes flux due to hydraulic gradient and vapour fluxes due to diffusion gradient. This formulation differs from Thomas & He (1997) in three aspects. First, the velocity of liquid  $\mathbf{v}_l$  includes thermal osmosis in addition to hydraulic gradient as per Darcy's law. Second, the diffusive flux term is cast in terms of the gradient of vapour mass. Third, vapour flux due to total gas pressure gradient is incorporated within the pore gas conservation equation.

The hydraulic conductivity relationship in Darcy's equation is given special attention in this study in order to accommodate highly swelling clays (Thomas *et al.*, 2003). The heat transfer equation employed follows the approach of Thomas & King (1991). The latent heat of vaporisation and specific heat capacities are a function of temperature.

A small-strain soil deformation theory is adopted, expressed in terms of a stress-strain equilibrium equation, following the approach proposed by Thomas & He (1997).

## EXPERIMENTAL WORK

In order to investigate the performance of the model, an experiment carried out by Commissariat à l'Énergie Atomique (CEA), France, on an MX80 bentonite column has been chosen (Gatabin & Billaud, 2005), with an initial relative humidity of 60%.

The characteristics of the MX80 sample after compaction are shown in Table 1. The experimental cell is shown in Fig. 1 (Gatabin & Billaud, 2005). A highly compacted cylindrical core of MX80 bentonite, 0.2027 m in diameter and 0.203 m high, was installed in the cell. Monitoring sensors were installed normal to the vertical axis. Measurements of temperature, relative humidity, radial stress and pore pressures were performed close to the axis of the column, whereas radial stress sensors were placed in contact with the outside surface of the sample. In addition, each cell was equipped

**Table 1. Characteristics of MX80 samples after compaction (Gatabin & Billaud, 2005)**

Property	Value
Powder conditioning, RH: %	60
Compaction pressure: MPa	33
Sample mass: g	13 332
Water content: %	13.66
Bulk density: g/cm <sup>3</sup>	2.035
Dry density: g/cm <sup>3</sup>	1.791
Porosity	0.3242
Degree of saturation	0.755

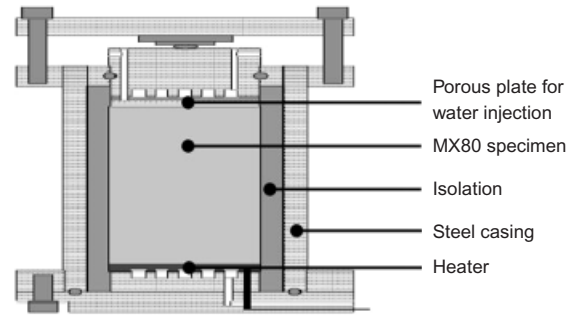


**Fig. 1. Schematic diagram of the thermo-hydraulic-mechanical cell (after Gatabin & Billaud, 2005)**

with a force sensor to measure the axial load. This sensor was located at the top of the sample.

The experiment was carried out in two phases. The first phase was a one-dimensional experiment and lasted up to 113 days. The material was subjected to a thermal load on the lower face of the cylinder, whereas the opposite face was kept at a constant temperature of 27.9°C. The thermal load was applied at 10°C per day below 100°C and 5°C per day above 100°C, with a maximum temperature of 150°C. In the second phase the temperature gradient was maintained and a constant 1 MPa water pressure was applied at the cold end, after the first phase approached equilibrium, that is, beyond 113 days.

## NUMERICAL SIMULATION

The numerical simulation was carried out using a two-dimensional, axisymmetric mesh consisting of 300 eight-noded quadrilateral elements. A rigorous investigation into the element size was conducted to ensure that the results this mesh produced were spatially converged. A time step of 100 s was considered, which was allowed to increase up to a period of 1 h, using an amplification factor of 1.05 whenever an increase was justified.

The initial uniform condition of the sample of 60% relative humidity corresponds to an initial pore water pressure of -70 MPa. The initial temperature was uniform at 22°C. The boundary conditions were applied in accordance with the experimental conditions.

The MX80 bentonite information pertaining to the moisture retention, hydraulic conductivity, thermal conductivity and air conductivity is based on Hökmark *et al.* (2005). Information regarding the deformation parameters is taken from Alonso *et al.* (1999), Villar (2003) and Sánchez *et al.* (2005). The key material properties are summarised in Table 2.

Comparisons of simulated and experimental results are presented for the evolution of temperature and relative humidity at different levels of the soil sample. Fig. 2 illustrates the temperature evolution with time at different levels of the sample, i.e. at 2.5 mm, 35 mm, 67.5 mm, 100 mm, 132.5 mm, 165 mm and 197.5 mm away from the heater. A good correlation can be seen between the two results. In phase 1 simulated temperature values are almost identical to the experiment. In phase 2 the temperature drops by approximately 2–3°C at locations near the heater end and the central region, compared with experimental results. This can be attributed to the lower thermal conductivity calculated by the model near the bottom half of the sample. Overall, the model results show excellent correlation. Heat transfer is predominantly affected by thermal conduction; thermal convection effects are limited, since moisture flow is relatively slow.

Figure 3 illustrates the evolution of relative humidity with

Table 2. Key material parameters

Property/relationship	Value/equation
Soil-water retention curve*	$S_l = \left[ 1 + \left( \frac{P_g - u_l}{P_0} \right)^{\frac{1}{1-\lambda}} \right]^{-\lambda} \cdot \left[ 1 - \left( \frac{P_g - u_l}{P_m} \right) \right]^{\lambda_m}$
Thermal conductivity*	$P_0 = 89 \text{ MPa}, \lambda = 0.38, P_m = 452 \text{ MPa}, \lambda_m = 1.0$ $\lambda = \lambda_{\text{dry}}(1 - S_l) + \lambda_{\text{sat}}S_l$ $\lambda_{\text{dry}} = 0.6, \lambda_{\text{sat}} = 1.3$
Unsaturated hydraulic conductivity (Hökmark, 2004)	$K_l = k_{\text{int}}K_{rl}/\mu_l, k_{\text{int}} = 1.5 \times 10^{-21} \text{ m}^2$ $K_{rl} = S_r^n, n = 3$
Air conductivity*	$K_g = k_{\text{int}}K_{rg}/\mu_g, K_{rg} = m(1 - S_r)$ $m = 1.0 \times 10^5$
Poisson's ratio, $\nu$	0.4
Thermal expansion coefficient, $\alpha_T$	$1.5 \times 10^{-4}/\text{K}$
Compressibility parameter for changes in net mean stress in elastic region, $\kappa$	0.0245
Compressibility parameter for changes in suction in elastic region, $\kappa_s$	0.075
$R_g$ , gas constant for pore gas (Geraminegad & Saxena, 1986)	$R_g = R_{da}(1 + 0.608S_w)$ $R_{da} = 1000 \text{ kg/m}^3$ $S_w = \text{weight fraction of water vapour in gas mixture}$
Molecular diffusivity of vapour species in air at reference temperature	$D_{\text{atms}} = 2.20 \times 10^{-5} \left( \frac{P_{\text{atm}}}{P_g} \right) \left( \frac{T}{T_0} \right)^{1.75}$
Saturated water vapour density for $T \leq T_{\text{crit}}$	$P_{\text{atm}} = 101325 \text{ Pa}, T_0 = 273.15 \text{ K}$ $\rho_0 = aT^6 + bT^5 + cT^4 + dT^3 + eT^2 + fT + g$ $a = -1.4374 \times 10^{-9}, b = 4.4243 \times 10^{-6}$ $c = -3.9280 \times 10^{-3}, d = 1.5910$ $e = -3.2258 \times 10^2, f = 3.2147 \times 10^4$ $g = -1.1546 \times 10^6$
Dynamic viscosity of water, $\mu_l$	$0.89 \times 10^{-3} \text{ Pa s}$
Density of water, $\rho_l$	$998 \text{ kg/m}^3$
$S_a$	$1 - S_l$

\* Akesson *et al.* (2005).

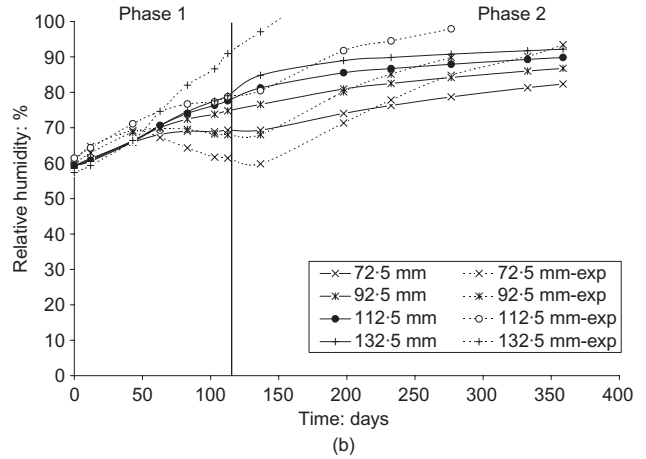
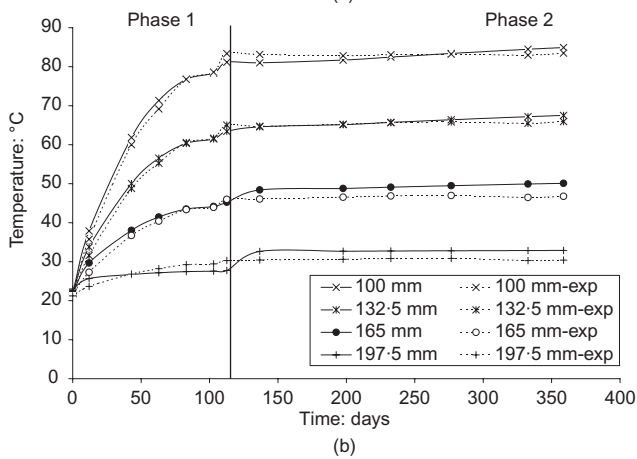
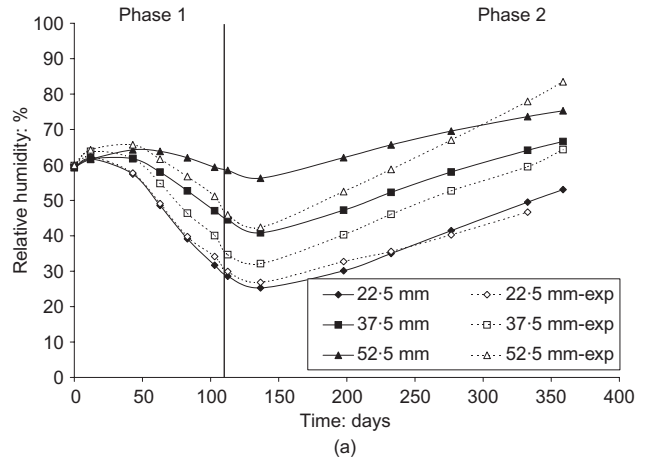
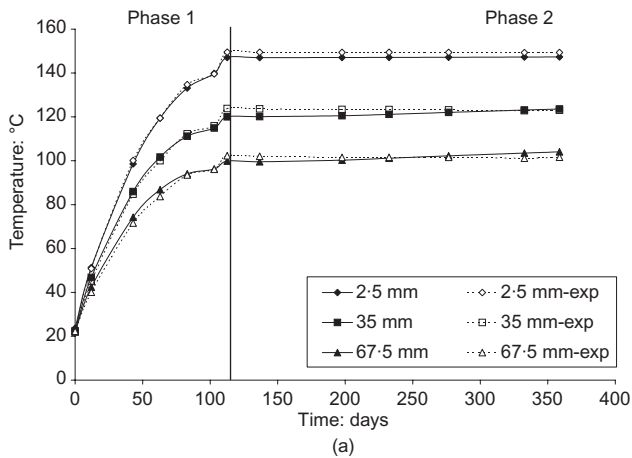


Fig. 2. Temperature evolution at: (a) 2.5, 35 and 67.5 mm; (b) 100, 132.5 and 197.5 mm away from the heater

Fig. 3. Relative humidity evolution at: (a) 22.5, 37.5 and 52.5 mm; (b) 72.5, 92.5, 112.5 and 132.5 mm away from the heater

time at different levels of the sample, that is, at 22.5 mm, 37.5 mm, 52.5 mm, 72.5 mm, 92.5 mm, 112.5 mm and 132.5 mm away from the heater. In phase 1, experimental values measured close to the heater surface show clearly the effects of evaporation, drying, with relative humidity reaching a low of 30% at the 22.5 mm location at 120 days. Condensation, wetting, causes a high of 90% relative humidity during the same period at 132.5 mm away from the heater. In phase 2, experimental values suggest resaturation at all the measured points with the sample reaching a high of 100% relative humidity in 150 days at 132.5 mm location.

For phase 1, the simulated relative humidity values compare well near the hot end and reasonably well away from the heater, that is, in the region 37.5–92.5 mm, notwithstanding some underestimation. The differences between experimental and numerical results yield a maximum difference, overestimation, of 15% at the 52.5 mm location, for example. This can be attributed to a slight overestimation of vapour flux in the region close to the heater, which causes condensation away from the heater during phase 1.

For phase 2, similar to experimental measurements, the simulated results show gradual resaturation at all the measured locations. The simulated relative humidity values compare well in the region 22.5–37.5 mm from the hot end. However, simulated results show a slower rate of resaturation compared with experimental results in the region 37.5–92.5 mm, although at the beginning of phase 2 the simulated results start off at higher relative humidity values than the experimental values. The slower rate of resaturation in this region is attributed to the temperature reaching highest values of 120°C, 100°C and 80°C at locations 35 mm, 67.5 mm and 100 mm respectively, as shown in Figs 2(a) and 2(b). Consequently, vapour flux is still active in this region, thus resisting a faster resaturation process.

## CONCLUSIONS

This note has presented a coupled thermo-hydro-mechanical model for unsaturated soil applicable for temperatures in excess of 100°C. The key advances included the development of a pore gas or bulk air transfer equation as opposed to dry air transfer, and modifications to the energy conservation equation via the incorporation of the effect of higher temperature on latent heat of vaporisation and specific heat capacities. The formulation for the moisture transport was modified to account for the manner in which pore gas equation was posed, that is, the inclusion of advective vapour transfer in the pore gas equation rather than the moisture transfer equation. Furthermore, provision was made to incorporate the effect of adsorbed water on the hydraulic conductivity. The performance of the model was illustrated via the simulation of a high-temperature (150°C) thermo-hydraulic-mechanical experiment, carried out on a column of MX80 bentonite by the Commissariat à l'Énergie

Atomique (CEA), France. The model exhibited good correlation with temperature results.

## REFERENCES

- Akesson, M., Birgersson, M., & Hökmark, H. (2005). *EBS task force benchmark calculations 1.1 and 1.2*. EBS Task Force, Barcelona.
- Alonso, E. E., Vaunat, J. & Gens, A. (1999). Modelling the mechanical behaviour of expansive clays. *Engng Geol.*, **54**, No. 1, 173–183.
- Gatabin, C. & Billaud, P. (2005). *Bentonite THM mock up experiments: Sensors data report*, Technical report NT DPC/SCCME 05–300A. Paris: CEA.
- Geraminegad, M. & Saxena, S. (1986). A coupled thermoelastic model for saturated-unsaturated porous media. *Géotechnique* **36**, No. 4, 539–550.
- Hökmark, H. (2004). Hydration of the bentonite buffer in a KBS-3 repository. *Appl. Clay Sci.*, **26**, Nos 1–4, 219–233.
- Hökmark, H., Ledesma, A., Lassabatère, T., Robinet, J.-C., Borgesson, L., Fälth, B. & Hernelind, J. (2005). *Temperature buffer test: Predictive modelling report*, SKB IPR-05–08. Stockholm: Swedish Nuclear Fuel and Waste Management.
- Luikov, A. V. (1966). *Heat and mass transfer in capillary porous bodies*. Oxford: Pergamon.
- Olivella, S., Gens, A., Carrera, J. & Alonso, E. E. (1996). Numerical formulation for a simulator (CODE\_BRIGHT) for the coupled analysis of saline media. *Engng Comput.* **13**, No. 7, 87–112.
- Olivella, S. & Gens, A. (2000). Vapour transport in low permeability unsaturated soils with capillary effects. *Transp. Porous Media*, **40**, No. 2, 219–241.
- Philip, J. R. & de Vries, D. A. (1957). Moisture movements in porous materials under temperature gradients. *Trans. Am. Geophys. Union*, **38**, No. 2, 222–232.
- Sánchez, M., Gens, A., Guimarães, L. & Olivella, S. (2005). A double structure generalized plasticity model for expansive materials. *Int. J. Numer. Anal. Methods Geomech.* **29**, No. 8, 751–787.
- Thomas, H. R. (ed.) (2006). *Opportunities, challenges and responsibilities for environmental geotechnics*, Proc. 5th Int. Conf. on Environmental Geotechnics, Cardiff **1** and **2**.
- Thomas, H. R. & He, Y. (1995). Analysis of coupled heat, moisture and air transfer in a deformable unsaturated soil. *Géotechnique* **45**, No. 4, 677–689.
- Thomas, H. R. & He, Y. (1997). A coupled heat-moisture transfer theory for deformable unsaturated soil and its algorithmic implementation. *Int. J. Numer. Methods Engng*, **40**, No. 18, 3421–3441.
- Thomas, H. R. & King, S. D. (1991). Coupled temperature/capillary potential variations in unsaturated soil. *ASCE J. Engng Mech.* **117**, No. 11, 2475–2491.
- Thomas, H. R., Cleall, P. J., Chandler, N., Dixon, D. & Mitchell, H. P. (2003). Water infiltration into a large-scale in-situ experiment in an underground research laboratory: physical measurements and numerical simulation. *Géotechnique* **53**, No. 2, 207–224.
- Villar, M. V. (2003). *AESPOE Hard Rock Laboratory, CIEMAT contribution to 2001*, Annual scientific report, CIEMAT/DIAE/54540/2/03. Madrid: CIEMAT.